# Symmetric Chaos

Mike Field and Martin Golubitsky

## A pictorial exploration of an order imposed by symmetry within chaotic systems

The possibility of order within chaos has been a driving force in much of the recent theory of dynamical systems. In this article we make a pictorial exploration of an order imposed by symmetry. In some ways the coexistence of chaotic dynamics and symmetric patterns may seem contradictory; but it is not, and the results of this marriage can be quite striking.

We begin by describing the very simple idea that we use to join symmetry and chaos. We choose a polynomial mapping $f:\mathbb{R}^2 \to \mathbb{R}^2$ and picture the attractors that are formed under iteration by f. We suppose that f commutes with a finite group $\Gamma$ of linear transformations and ask how this symmetry affects the kinds of attractors we find. As shown in Reference 1, we expect to find, for certain f, attractors that are invariant under all of the transformations in $\Gamma$.

Pictures such as those in Figs.1–3 are formed as follows. We fix $\Gamma$ and f (in a way that is explained in Section 1). Then we choose an initial point $x_0$ and iterate f until the transients die away. Letting f iterate and plotting the points on the resulting orbit yields a picture of the 'attractor.' The black and white images are formed in this way. For the color pictures, we count the number of times each pixel is hit during the iteration process and color by number. This process gives a representation of the density function for the invariant measure on the attractor.

In this article we discuss both the symmetry groups that can be used in the plane and the simplest symmetric maps. We discuss the coloring program that we have developed—noting that different colorings bring out different structures on the attractor. We shall even discuss how it is possible to develop symmetric fractals using iterated function systems[2]. Finally, we discuss a potential application.

*Mike Field is a Reader in mathematics at Sydney University. His main interests are equivariant dynamical systems, symmetry breaking bifurcations and the use of interactive computer graphics in the study of nonlinear systems. Martin Golubitsky is Cullen Professor of Mathematics at the University of Houston. His main interests lie in bifurcation theory and its applications, especially to systems with symmetry.*

In a more theoretical direction, it has been shown in Reference 3 that it is possible to have static equivariant bifurcations to periodic phenomena in low dimensional systems of ODE. In related work, strong numerical evidence has been obtained indicating direct bifurcation from steady states to chaotic dynamics in equivariant systems, where the chaotic attractor has nontrivial symmetry. It is hoped that this work will lead to a better understanding of the mechanisms leading to this type of chaotic dynamics.

### Section 1: Symmetry Groups and Symmetric Mappings

The only finite groups of linear transformations that act on the plane are the dihedral groups $\mathbb{D}_n$ of symmetries of the regular n-gon and the cyclic subgroups $\mathbb{Z}_n$ of $\mathbb{D}_n$ consisting of the orientation-preserving symmetries. Polynomial mappings of the plane that commute with these

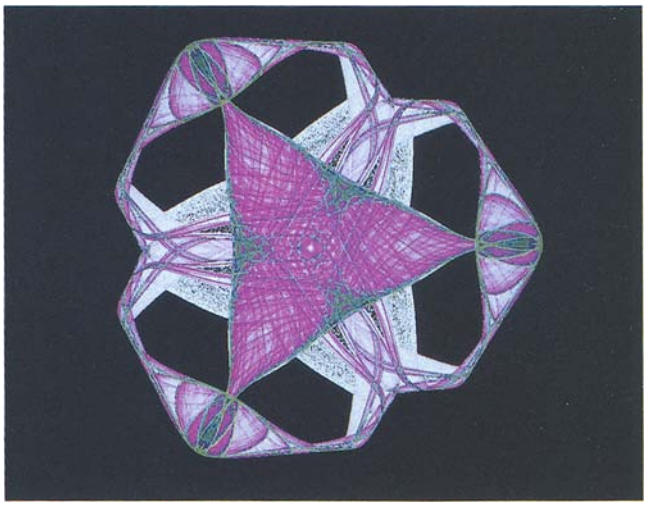

**Fig.1: Attractor of mapping (1a) with n=3; $\lambda=1.56$; $\alpha=-1.0$; $\beta=0.10$; $\gamma=-0.82$; $\delta-0.05$; p=3.**

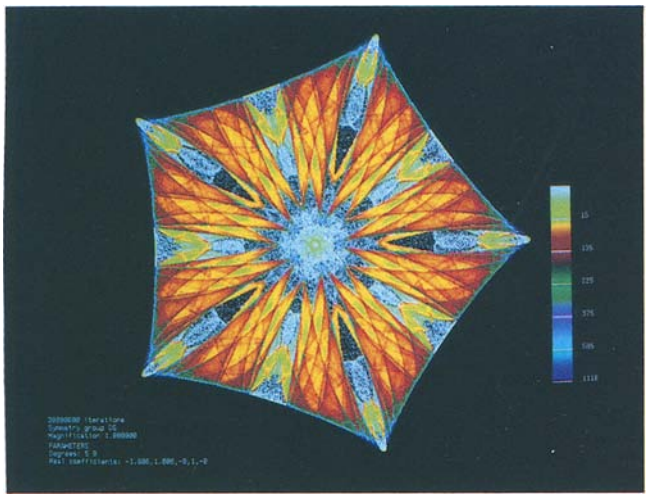

**Fig.2: Attractor of mapping (1a) with n=5; $\lambda=-1.806$; $\alpha=1.806$; $\beta=0$; $\gamma=1$.**

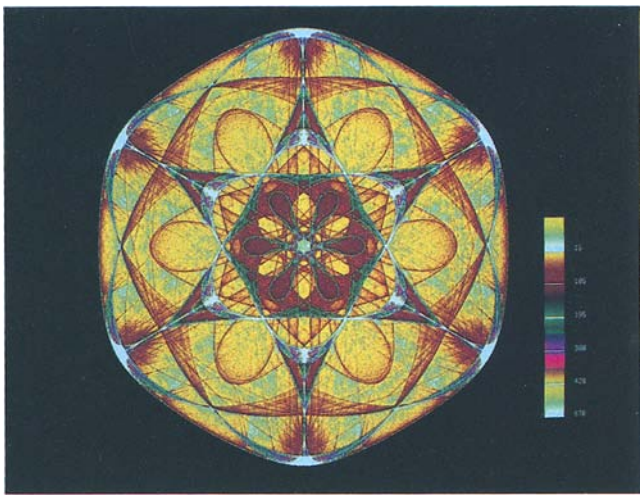

**Fig.3: Attractor of mapping (1a) with n=6; $\lambda=-2.7$; $\alpha=5.0$; $\beta=2.0$; $\gamma=1.0$.**

symmetry groups are given in complex coordinates as follows.

Let $u = z\bar{z}$ and $v = z^n$. Then polynomial mappings $f:\mathbb{C}\to\mathbb{C}$ that commute with $\mathbb{D}_n$ have the form:

$$f(z) = p(u,\mathrm{Re}(v))z + q(u,\mathrm{Re}(v))\bar{z}^{n-1}$$

where p and q are arbitrary real-valued polynomials. Most of the attractors in this article are formed using the truncated form:

$$f(z) = (\lambda + \alpha u + \beta\,\mathrm{Re}(v))z + \gamma\bar{z}^{n-1} \qquad (1a)$$

where $\lambda, \alpha, \beta, \gamma$ are real constants. Indeed, the basic phenomena seen in these mappings occur already when $\beta = 0$; the resulting three-parameter family can then be scaled to two parameters:

$$f(z,\ \lambda,\ \gamma) = \lambda(1-u)z + \gamma\bar{z}^{n-1}. \qquad (1b)$$

The two-parameter family Eq. (1b) may be thought of as the odd logistic equation—the $\lambda(1-u)z$ term—which leaves each radial line invariant and an $0(2)$ symmetry breaking term $\gamma\bar{z}^{n-1}$. The one-dimensional odd logistic equation $\lambda(1-x^2)x$ has been well studied by Hao Bai-Lin[5].

Similarly, we can describe polynomials that commute with $\mathbb{Z}_n$ rather than $\mathbb{D}_n$. These mappings have the form:

$$f(z) = p(u,v)z + q(u,v)\bar{z}^{n-1}$$

where p and q are arbitrary complex-valued polynomials. In our numerical exploration of $\mathbb{Z}_n$ symmetry we have added just one term $i\omega z$ to yield:

$$f(z) = (\lambda + \alpha u + \beta\,\mathrm{Re}(v) + \omega i)z + \gamma\bar{z}^{n-1}. \qquad (1c)$$

For $\omega \neq 0$, Eq. (1c) is $\mathbb{Z}_n$ symmetric but not $\mathbb{D}_n$ symmetric. Varying $\omega$ in Eq. (1c) from zero to non-zero values allows us to see the effect of breaking symmetry from $\mathbb{D}_n$ to $\mathbb{Z}_n$.

In our investigation of maps with $\mathbb{D}_n$ symmetry, we have sometimes added an extra term:

$$f(z) = (\lambda + \alpha u + \beta\,\mathrm{Re}(v))z + \gamma\bar{z}^{n-1} + \delta(\mathrm{Re}(z/|z|)^{np}z|z| \qquad (1d)$$

This term is not polynomial, having a mild singularity at the origin. In particular, for non-zero $\delta$ this term tends to dominate the iteration near $z = 0$.

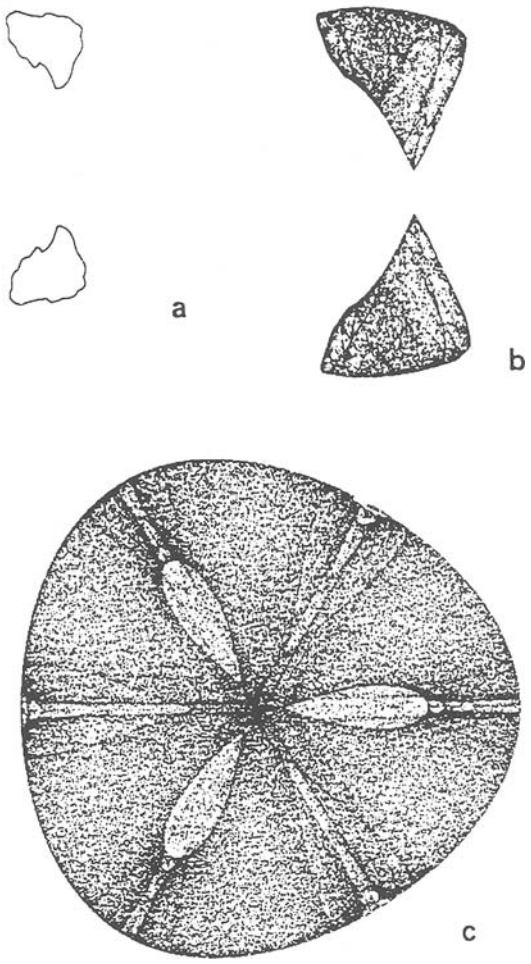


**Fig.4: Symmetry creation. Attractors of mapping (1a) with n=3; $\alpha=1.0$; $\beta=0.0$; $\gamma=0.1$. (a) $\lambda=-2.10$; (b) $\lambda=-2.25$; (c) $\lambda-2.38$. Transitions occur at $\lambda$ approximately $-2.12$ and $-2.375$.**

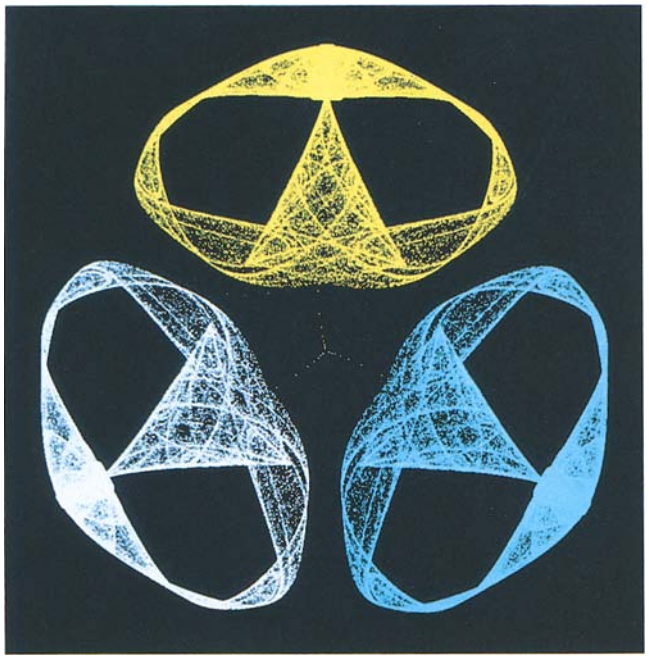

**Fig.5: Conjugate attractors (shown in different colors) of mapping (1a) with n=3; $\lambda=1.5$; $\alpha=-1.0$; $\beta=0.1$; $\gamma=-0.8$.**

Mathematically, the two most noteworthy phenomena associated with attractors obtained from these mappings are that the attractors can have full symmetry (either $\mathbb{D}_n$ or $\mathbb{Z}_n$ depending on whether or not $\omega$ is zero), and, as a parameter is varied, attractors with less symmetry can suddenly bifurcate to attractors with greater symmetry. Both of these phenomena are described in Reference 1.

An example of *symmetry creation* is given in Fig.4, where the bifurcation parameter $\lambda$ is the coefficient of the linear term. As $\lambda$ decreases from $-0.9$ we see: a period-doubling bifurcation, then a Hopf bifurcation to invariant circles, Fig.4(a); a breakdown of the invariant curves to a strange attractor, Fig.4(b); and then a merging of conjugate attractors to form one fully symmetric attractor, Fig.4(c). In Fig.5 we show, for a different set of parameters, the three conjugate attractors (corresponding to three different initial conditions) in three different colors.

In Fig.6 we show the symmetry-breaking effect on the attractor that may be found by adding a small rotation $\omega$, as in Eq. (1c). The difference between $\mathbb{D}_n$ symmetry and $\mathbb{Z}_n$ symmetry (where $n=16$) can be clearly seen in this figure.

In Fig.7(a) we illustrate the effect of adding the non-polynomial term $\delta$ by using an example with 9-fold symmetry. The addition of such terms typically adds more structure near the origin. We illustrate this phenomenon in Fig.7(b) by showing a 20-fold magnification of a square neighborhood of the origin.

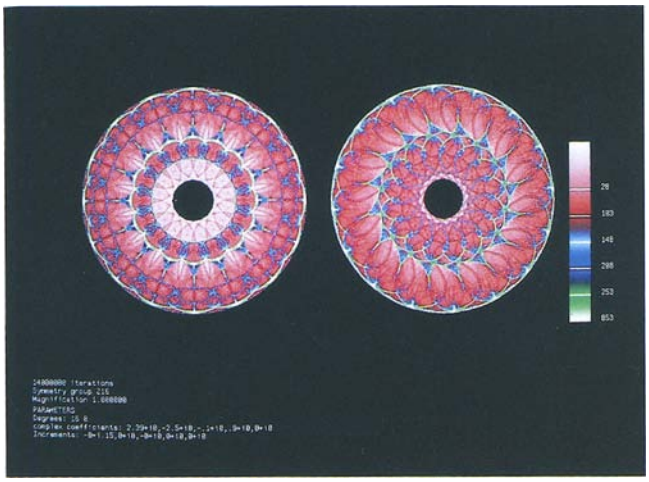

**Fig.6: The effect of breaking symmetry from $D_{16}$ to $Z_{16}$. Attractor of mapping (1c) with n=16; $\lambda=2.39$; $\alpha=-2.5$; $\beta=-0.1$; $\gamma=0.9$. The two pictures are with $\omega=0.0$ and $\omega=-0.15$.**

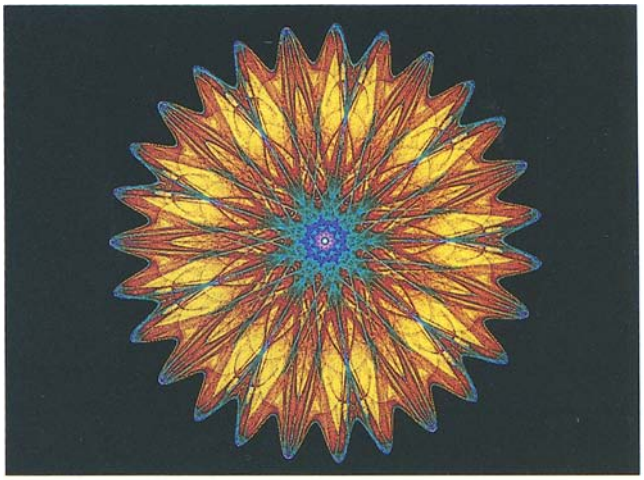

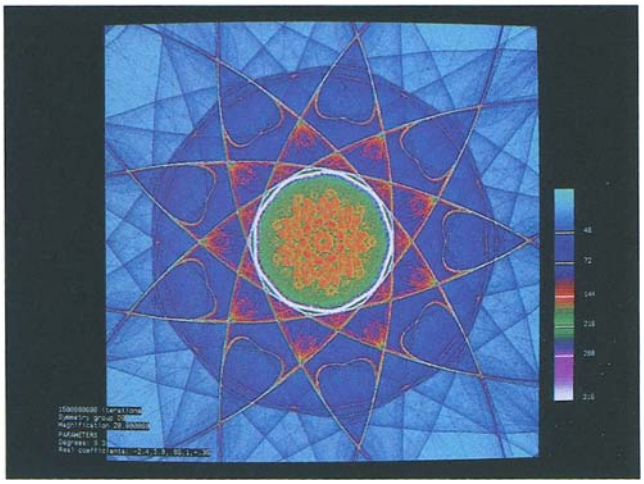

**Fig.7: Scaling of structure in map (1d) with non-zero delta. (a) (upper) Attractor with n=9; $\lambda=-2.4$; $\alpha=3.8$; $\beta=0.85$; $\gamma=1.0$; $\delta=-0.35$; p=3. (b) (lower) Attractor magnified 20 times near origin.**

Recently, in cooperation with Ian Stewart, we have begun to explore a second kind of symmetric mapping whose attractors can be visualized in the plane: the torus mapping (see Fig.8). There are two advantages to using torus maps. Firstly, since tori are compact, iterates of torus maps always remain bounded; and secondly, the attractors of torus maps, when viewed in the plane, can be repeated periodically (see Fig.9) to form interesting quilt-like patterns. Several examples are given in Fig.10.

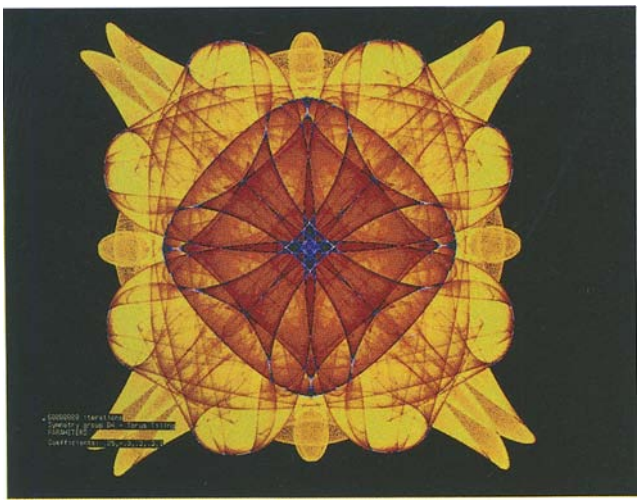

**Fig.8: Attractor of torus mapping (1f) with $\lambda=0.25$; $\alpha=-0.3$; $\beta=0.2$; $\gamma=0.3$; $k=1$.**

We view the torus $\mathbb{T}^2$ as $\mathbb{R}^2/\mathscr{L}$ where $\mathscr{L}$ is a planar lattice. Then mappings $g:\mathbb{T}^2\to\mathbb{T}^2$ can be lifted to mappings $f:\mathbb{R}^2\to\mathbb{R}^2$ of the form $f(X)=p(X)+L(X)$ where p is doubly periodic (that is, $p(X+\ell)=p(X)$ for all $\ell\in\mathscr{L}$) and L is a linear map that preserves $\mathscr{L}$. To introduce symmetry, we require that the mappings g (and hence f) commute with the linear symmetries (or *holohedry*) of the lattice. We perform the iteration of the torus map g by iterating the lifted mapping f modulo $\mathscr{L}$.

Specifically, we consider here only the square lattice of unit length. Thus periodicity reduces to $p(x+1,y)=p(x,y+1)=p(x,y)$; and the holohedry is $\mathbb{D}_4$, the symmetries of the square. These symmetries are generated by $(x,y)\to(y,x)$ and $(x,y)\to(1-x,y)$. Commutativity with respect to $\mathbb{D}_4$ implies that:

$$f(x,y)=p(x,y)+k(x,y) \qquad (1e)$$

where $k\in Z$ and the periodic map $p=(p_1,p_2)$ has the form:

$$p_2(x,y)=p_1(y,x)$$

and:

$$p_1(x,y)=\Sigma\ a_{mn}\cos(2\pi mx)\sin(2\pi ny).$$

The specific mapping whose attractors we have explored is as follows:

$$f(x,y)=\lambda\begin{pmatrix}\sin(2\pi x)\\ \sin(2\pi y)\end{pmatrix}+\alpha\begin{pmatrix}\sin(2\pi x)\cos(2\pi y)\\ \sin(2\pi y)\cos(2\pi x)\end{pmatrix}$$

$$+\beta\begin{pmatrix}\sin(4\pi x)\\ \sin(4\pi y)\end{pmatrix}+\gamma\begin{pmatrix}\sin(6\pi x)\cos(4\pi y)\\ \sin(6\pi y)\cos(4\pi x)\end{pmatrix}+k\begin{pmatrix}x\\ y\end{pmatrix}. \qquad (1f)$$

Finally, we refer the reader to the very recent preprint by King and Stewart which develops some of the themes discussed in this work.[6]

## Section 2: Using Symmetry to Visualize Chaos

Iterates of $\mathbb{D}_n$ symmetric mappings in the plane provide a simple way to visualize the signature of chaos—sensitive dependence on initial conditions. First note that the lines generated by the $n^{th}$ roots of unity in the complex plane are invariant under iteration by $\mathbb{D}_n$ symmetric mappings. This can be seen by direct calculation or, more generally, using fixed-point subspace arguments (see Reference 4, Chapter XII). When one looks at the pictures of symmetric chaos shown previously, this fact seems rather remarkable, since the lines of symmetry appear to have nontrivial intersection with the trajectory that forms the attractor. It follows from symmetry, however, that if an iterate ever lands on an axis of symmetry, then all subsequent iterates remain on that axis.

The existence of lines of symmetry allows us to divide the attractor into 2n pieces, obtained by intersecting the attractor with the 2n wedges in the complement of the lines of symmetry. For the remainder of our discussion we restrict our attention to triangular symmetry ($n=3$).

During the iteration process we can determine the wedge in which a given iterate lies. This allows us to make a color description of the mapping, as follows. We assign to each of the six wedges a different color, as shown in the border of Fig.11. We then color each pixel on the screen according to which wedge that pixel ends up in after

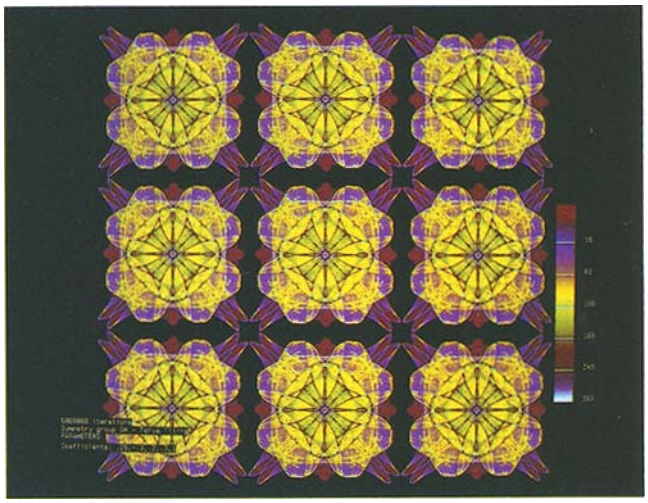

**Fig.9: Same attractor as in Fig.8 repeated periodically on a 3x3 grid.**

iteration by f. This explains the colors used in the interior of Fig.11. For comparison, we show in Fig.12 the $\mathbb{D}_3$ symmetric attractor associated with the mapping in Fig.11.

Note that the $\mathbb{D}_3$ symmetry of this mapping is apparent in the coloring of Fig.11. That is, the coloring in each wedge can be obtained from the coloring in one wedge by rotating the colors of the boundary as one rotates the wedges. There is, of course, an ambiguity in the coloring of Fig.11 associated with the question of precisely which point inside a given pixel is iterated. Different points may iterate to different wedges, and hence determine different colors for the whole pixel; we ignore that issue here.

We now show how we can get a series of color pictures that illustrate sensitive dependence on initial conditions for this $\mathbb{D}_3$ symmetric mapping. Suppose we color a pixel by determining in which wedge the second iterate lies, as we have done in Fig.13(a). What we find is

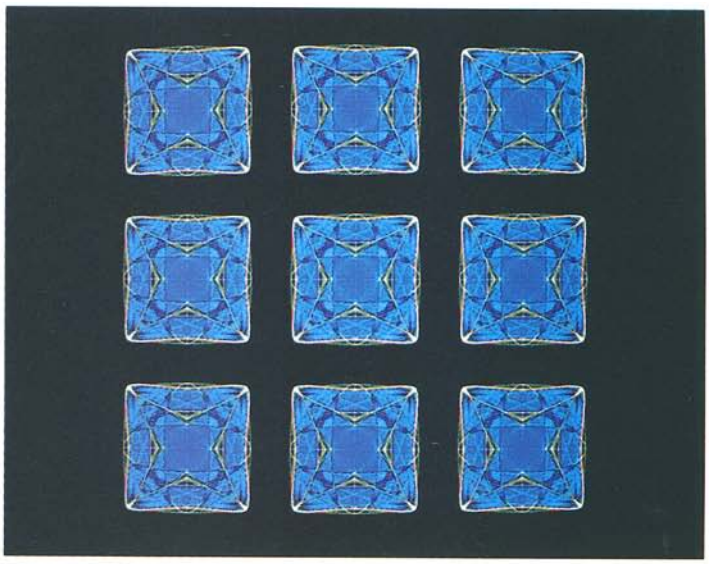

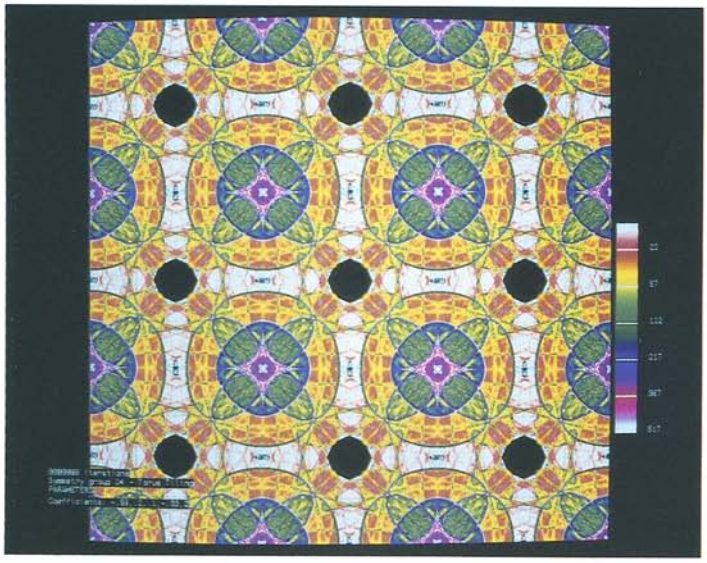

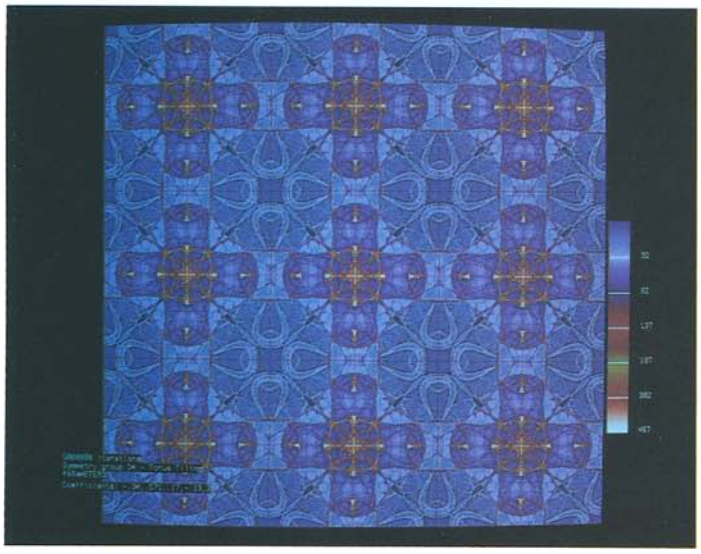

**Fig.10: Quilt patterns. Attractors of torus mapping (1f). *(a) (top) $\lambda=-0.59$; $\alpha=0.2$; $\beta=0.1$; $\gamma=-0.09$; $k=0$. (b) (center) $\lambda=-0.59$; $\alpha=0.2$; $\beta=0.1$; $\gamma=-0.33$; $k=2$. (c) (bottom) $\lambda=-0.34$; $\alpha=0.571$; $\beta=0.17$; $\gamma=-0.13$; $k=2$.**

that the colors begin to mix. Indeed, when we color the eighth iterate it is obvious that points in neighboring pixels are being rapidly mixed by the iteration process. This mottling gives a striking representation of sensitive dependence on initial conditions.

It is worth remarking that the chaotic dynamics pictured using these $\mathbb{D}_n$ symmetric mappings of the plane could not have existed had we restricted our attention to invertible maps. A simple continuity argument, coupled with the invariance of the lines of symmetry, shows that connected wedges have to map to connected wedges; that is, symmetric chaos is not possible. It is possible, however, to obtain this kind of symmetry creation and symmetric

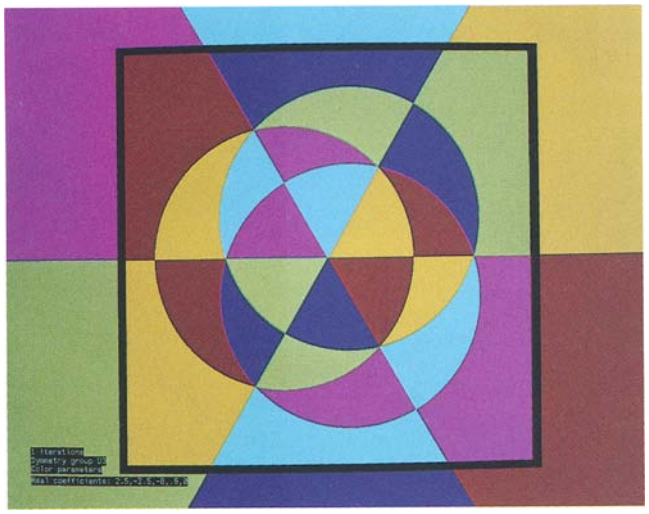

**Fig.11: Color coding of sensitive dependence on initial conditions using mapping (1a) with n=3; λ=2.5; α=−2.5; β=0.0; γ=0.9. One iterate in advance.**

chaos for invertible mappings, if one looks in higher dimensions. In particular, the pictures of the attractors associated with these $\mathbb{D}_n$ symmetric mappings could have been obtained by projecting the attractor of an invertible $\mathbb{D}_n$ symmetric mapping on $\mathbb{R}^4$ into the plane. This observation is important when considering applications that are governed naturally by systems of differential equations, which generate invertible mappings.

## Section 3: Symmetric Fractals

Our previous discussion focused on how symmetry can be introduced into the study of chaotic dynamics. We now make an analogous statement for the study of fractals using the notion of iterated function systems[2].

Iterated function systems provide a simple way for generating fractals in the plane, as follows. Choose a collection of k contracting affine mappings $\rho_j$. Recall that an affine map has the form $\rho(X) = LX + b$ where L is an invertible matrix and b represents a translation. The affine map is a *contraction* if L is a contraction, that is, if all of the eigenvalues of L have modules less than unity. The collection $\{\rho_1,\ldots,\rho_k\}$ is an *iterated function system* if each affine map $\rho_j$ is a contraction.

Next, form the following dynamical process. Choose an initial point $x_0$ and (with a uniform distribution) randomly choose a map $\rho_j$. Let $x_1 = \rho_j(x_0)$. Now, randomly choose another j and form $x_2$, etc. Since the $\rho_j$ are contractions this process will, with probability 1, form a bounded sequence. Indeed, the process has a unique attractor A that is characterized by the set theoretic formula (see Barnsley[2])

$$A = \bigcup_{j=1}^{k} \rho_j(A). \tag{3a}$$

We now form an iterated function system in a slightly different way. Choose one affine contraction $\rho$ and a symmetry group $\Gamma$ of order k. Then form an iterated function system by setting $\rho_j = \gamma_j \rho$ where the $\gamma_j$ are the elements of $\Gamma$. It follows from Eq. (3a) that the resulting attractor A has to be $\Gamma$ symmetric. Examples of such fractals are given in Fig.14. As before, the coloring represents the invariant measure on A.

## Section 4: Prism

The programs we describe here are part of a package that we have named *Prism* (a mnemonic for PRograms for the Interactive Study of Mappings). The two main programs included in *Prism* are *iter*, which iterates maps and produces data files, and *draw*, which reads the data files produced by *iter* and colors the attractor.

The primary purpose of *iter* is the rapid computation of large numbers of iterates (typically between 20 and 150 million) and the storing of the resulting pixel hit information in a data file. As well as this facility for producing data files, *iter* can be used interactively to examine and display iterations and to study the effects of incrementing parameters. In this mode it is possible to display between 1 and 20 plots on the screen and to edit and save parameters. Normally, such plots are done using

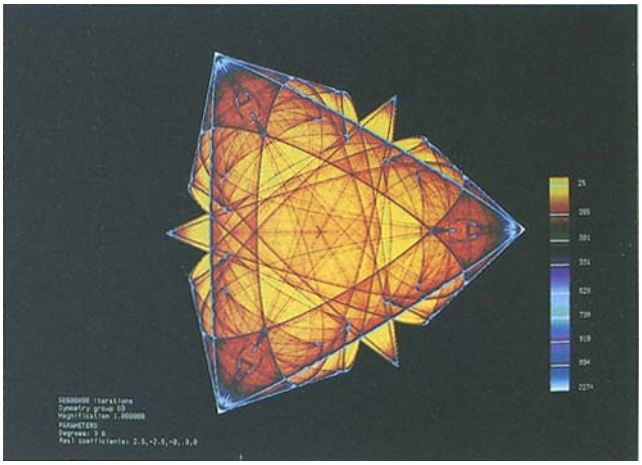

**Fig.12: Attractor for mapping in Fig.11.**

between 5,000 and 50,000 iterations per plot. An important benefit of this procedure is the possibility of seeing new kinds of bifurcations related both to the shape of the attractors and to the structure of the invariant measures on the attractors. In Fig.15 we present an example with $D_7$ symmetry where each of the attractors has full symmetry but changes in the geometric structure of the attractor occur.


**Fig.13: Color coding as in Fig.11. (a) (upper) 4 iterates in advance. (b) (lower) 8 iterates in advance.**

*Draw* has to be flexible enough to meaningfully color attractors with large variations in the number of pixel hits, and easy enough to operate so that it is possible to tinker with the colors. For example, if we let max_hit denote the maximum number of times any individual pixel is hit, we typically find that 93% of the pixels are hit between 1 and (max_hit/500) times and 99% between 1 and (max_hit/100) times. This phenomenon is perhaps not so surprising: in any visual image (a mountain range or a face) much of the significant information (ridges or creases) is supported on a very small area, a fact well-known to artists.

Generally, the features associated to pixels with a large number of hits are relatively easy to locate and display. Features associated with a small number of hits require extra resolution. In our context we obtain more resolution by increasing the number of iterations. Fig.16(b) shows the same attractor with 16 times as many iterates as Fig.16(a).

For a successful color editor one needs to work with as few variables as possible; however, the more colors one uses the greater the resolution one can expect. We adopted the following strategy for coloring. Rather than working with individual colors, we work with color bands. Each color band may be regarded as a linear segment in RGB-space, where we specify the initial and final colors and the number of intermediate points. To color an attractor, we

start by selecting a small number of color bands and a range in pixel hits for each band—say all pixels with pixel hits in the range $(0,g_1]$ will be colored by band 1 and all pixels with pixel hits in the range $(g_1,g_2]$ will be colored by band 2, etc. If we divide band 1 into k sub-intervals then we assume that the initial color is assigned to pixels with pixel hits between 1 and $INT(g_1/k)$, etc. Generally, we use between 4 and 7 color bands and divide each color band into approximately 15 sub-bands. We find that reasonable colorings require 70 to 100 colors. The program has a feature that allows it to store successful color bandings.

In Fig.17 we show the same attractor with two different color strategies: the first uses two bands and 30 colors, while the second uses 5 bands and 100 colors.

Various options come with *draw* that allow one, for example, to devote the entire screen to the attractor. We use this feature for taking photographs of the images. In this way it is possible to get high-quality output rather inexpensively. The pictures for this article were taken from a SUN high-resolution color monitor using Kodachrome EPR-64 professional quality film.

Both *iter* and *draw* were written in C and utilize various system calls (such as compression, file copying and removal). The iteration part of *iter* uses an optimized version of complex multiplication that runs 1.5 to 2 times faster on computing complex powers than does the standard induction definition.

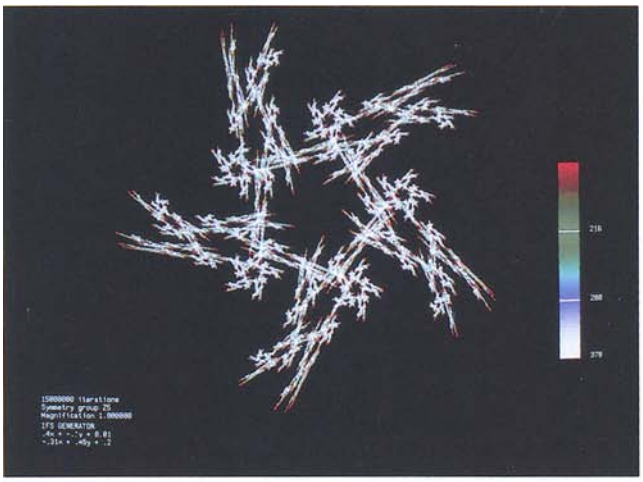

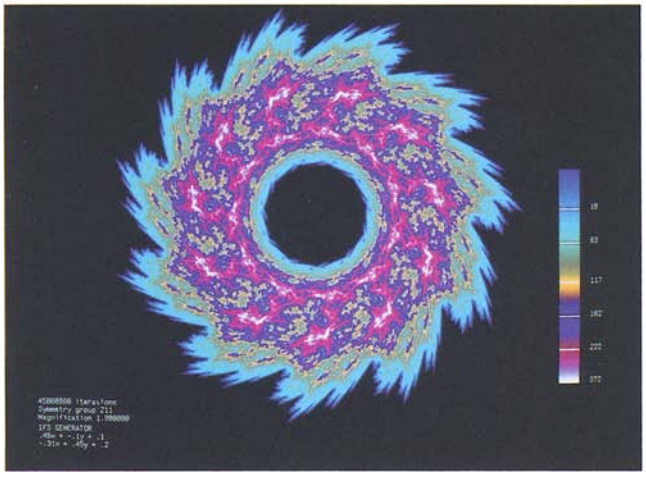

**Fig.14: Symmetric fractals. Attractors using symmetric iterated function systems. (a) (top) Affine map $(0.40x-0.1y+0.01, -0.31x+0.45y+0.2)$; symmetry $Z_5$. (b) (center) Affine map $(0.40x-0.1y+0.01, -0.35x+0.40y+0.2)$; symmetry $D_9$. (c) (bottom) Affine map $(0.45x-0.1y+0.10, -0.31x+0.45y+0.2)$; symmetry $Z_{11}$.**

## Section 5: Applications

The major application that we foresee for symmetry-increasing bifurcations is to provide an explanation for certain forms of patterned turbulence in hydrodynamics. As mentioned in Reference 1, a good candidate for such a

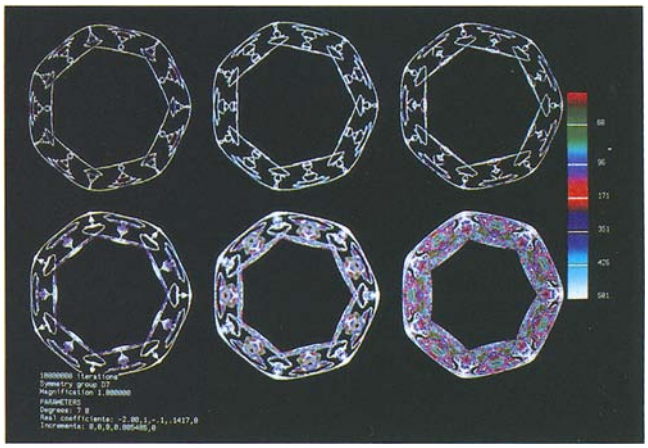

**Fig.15: Bifurcation diagram of attractors of mapping (1a) with $n=7$; $\lambda=-2.08$; $\alpha=1.0$; $\beta=-0.1$; $\gamma=0.1417$. Gamma is incremented by 0.005485 between pictures.**

correlation is the turbulent Taylor vortex state in the Couette-Taylor apparatus. This apparatus consists of a fluid contained between two independently rotating cylinders.

What is observed in the experiments when the outer cylinder is held fixed and the speed of the inner cylinder, or *Reynold's number*, is increased slowly, is a first transition from laminar flow to a flow—called *Taylor vortices*—that has a cellular structure with an exactly straight cell boundary and that can be related to invariance under a reflectional symmetry across a plane perpendicular to the cylinder axis, as well as to the

rotational symmetry of the apparatus. Subsequent bifurcations maintain the cellular structure but break the symmetry.

Eventually, at relatively high speeds of the inner cylinder where turbulent fluid motion has begun, the straight cellular structure reasserts itself, at least on average. What is meant by 'on average' is that, if a time series of the fluid flow field were time-averaged, then the straight boundary between cells would be exact. As it is, of course, the fluid does flow across the cell boundary, but rather more slowly than the fluid velocity would suggest.

We believe that a symmetry-increasing bifurcation of chaotic attractors has taken place in the Navier-Stokes equations. However, neither direct analytic nor numeric exploration of this state is currently possible. Our reasoning is that if such a bifurcation did occur, then before the bifurcation the flow would be asymmetric on average, but afterwards it would be symmetric. Here we are thinking of our mapping as a time $\Delta t$ map associated with the flow of the Navier-Stokes equations. Much work, including specifying a more precise bifurcation, is needed before we can actually claim to understand this potential application.

Acknowledgements: Development of the programs used to produce the pictures in this article was initiated in collaboration with Jim Richardson (Sydney) in 1988. Preliminary versions of the software were run on Apollo Domain color workstations, with most of the heavy computation done on an Apollo 10000 super-minicomputer. Subsequent development of the programs has been on SUN SPARC stations at the Center for Applied Mathematics, Cornell University, New York, and the

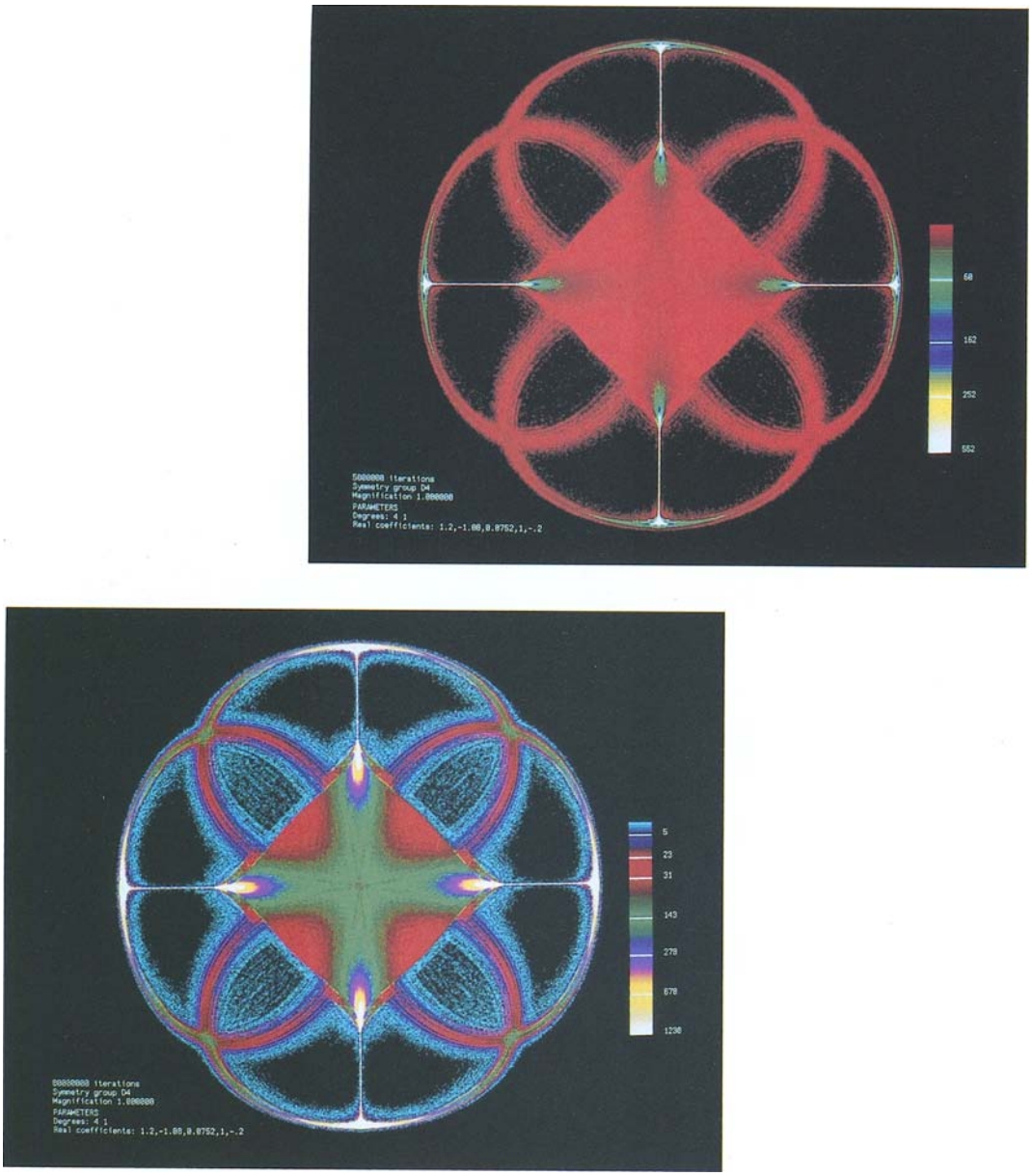


**Fig.16: Attractor of mapping (1d) with $n=4$; $\lambda=1.2$; $\alpha=-1.0$; $\beta=0.0752$; $\gamma=1.0$; $\delta=-0.2$. (a) (upper) 5 million iterates. (b) (lower) 80 million iterates.**

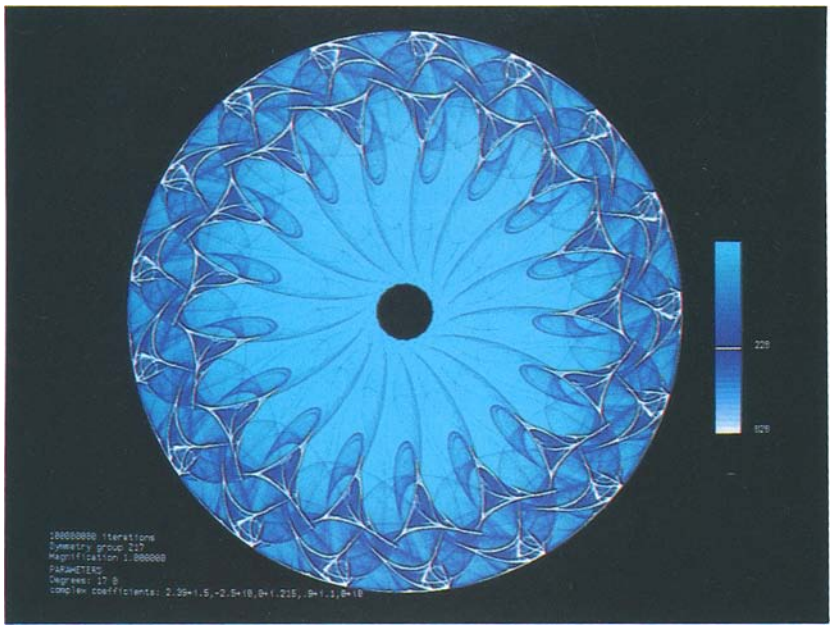


**Fig.17: Enhancement of structure by changes in color.**

Department of Mathematics, University of Houston, Texas.

We have profited from discussions with many individuals concerning the topics discussed in this paper. In particular, we wish to thank Ian Stewart for his help in initiating the study of quilt-like patterns using torus maps, and Martin Krupa for his suggestion to investigate symmetry-breaking from $D_n$ to $Z_n$ symmetry.

We would also like to acknowledge help we have received from several sources. Pitt Research of Sydney gave us advice on color enhancement techniques related to satellite photography. William Reeves of Pixar advised us about anti-aliasing techniques which we have incorporated into some of our software. Apollo Domain (Australia) gave financial support for the production of hard-copy. The research of MG was supported in part by NSF/DARPA (grant DMS-8700897) and the Texas Advanced Research Program (ARP-1100). The research of MF was supported in part by the U.S. Army Research Office, through the Mathematical Sciences Institute of Cornell University. Last, but by no means least, special thanks are due the Center for Applied Mathematics, Cornell University, for the use of their computing facilities and for providing such a stimulating and helpful environment.

## References

1. P. Chossat and M. Golubitsky, "Symmetry-increasing bifurcation of chaotic attractors." *Physics D* **32** (1988) 362–392.
2. M. Barnsley, *Fractals Everywhere*, Academic Press, Boston, 1988.
3. M. Field and J. W. Swift, "Stationary bifurcations to limit cycles and heteroclinic cycles." *J. Nonlinear Science.* Submitted.
4. M. Golubitsky, I. N. Stewart and D. G. Schaeffer, *Singularities and Groups in Bifurcation Theory: Vol. II,* Appl. Math. Sci. **69**, Springer-Verlag, New York, 1988.
5. Hao Bai-Lin, *Elementary Symbolic Dynamics,* World Scientific, Singapore, 1989.
6. G. King and K. Stewart, "Symmetric Chaos," preprint, Nonlinear Systems Lab, University of Warwick, UK, 1990.